SELECTION AND EVALUATION OF MODELS FOR SUBSTANTIALLY COMPLETE CONTAINMENT EXAMPLE PROBLEM

Prepared for

Nuclear Regulatory Commission
Contract NRC-02-88-005

Prepared by

Narasi Sridhar

Center for Nuclear Waste Regulatory Analyses
San Antonio, Texas

September 1992

PREVIOUS REPORTS IN SERIES

Number	Name	Date Issued
NUREG/CR-5638	Technical Considerations for Evaluating Substantially Complete Containment of High-Level Waste Within the Waste Package	December 1990
NUREG/CR-5639	Uncertainty Evaluation Methods for Waste Package Performance Assessment	January 1991
CNWRA90-007	"Substantially Complete Containment" Feasibility Assessment and Alternatives Report	September 1990

ABSTRACT

This is an intermediate milestone report evaluating the models that will be used in an example analysis of the feasibility of a quantitative evaluation of "Substantially Complete Containment" requirement in Code of Federal Regulations (CFR) Title 10 Part 60.113. The models for corrosion potential; pit initiation, growth and repassivation; crevice corrosion initiation, growth and repassivation; stress corrosion cracking; buckling; and fast fracture are evaluated. Simple parametric equations for the critical potentials associated with these phenomena are suggested. An overall approach for the example analysis is outlined.

CONTENTS

CONTENTS (cont'd)

FIGURES

ACKNOWLEDGMENTS

This report was prepared to document work performed by the Center for Nuclear Waste Regulatory Analyses (CNWRA) for the U.S. Nuclear Regulatory Commission (NRC) under Contract No. NRC-02-88-005. The activities reported here were performed on behalf of the NRC Office of Nuclear Material Safety and Safeguards, Division of High-Level Waste Management. The report is an independent product of the CNWRA and does not necessarily reflect the views or regulatory position of the NRC.

Discussions with Drs. J. Walton, G. Cragnolino, and R. Manteufel are gratefully acknowledged. Dr. G. Cragnolino provided the input to the section on stress corrosion cracking. Dr. P. Nair provided input to the section on mechanical failures.

1 EXECUTIVE SUMMARY

An approach to the analysis of the feasibility of a quantitative definition of "Substantially Complete Containment" in 10 CFR 60.113 is outlined in this report. The approach consists of modeling the corrosion potential of a container material as a function of time for various environmental conditions and comparing this to critical potentials for various corrosion phenomena such as pitting, crevice corrosion, and stress corrosion cracking. For the corrosion models, the containers are assumed to come into contact with an aqueous environment. The containers which are exposed only to dry conditions are assumed to be uncorroded. A simplified model for corrosion potential of a thin-walled container made of type 304/304L stainless steel is recommended. This model is based on an analysis of coupled charge-transfer and transport processes occurring at the container surface. The uncertainties in the input parameters for the corrosion potential model are discussed. The models for pitting, crevice corrosion, and stress corrosion cracking that are available for the purpose of the example analysis are reviewed briefly. Simple parametric equations for predicting the critical potentials as a function of major environmental factors, such as chloride concentration and temperature, are recommended. Simple analysis of mechanical failure modes, buckling and overload fracture, are suggested and their limitations are pointed out.

2 AN APPROACH TO QUANTIFICATION OF SUBSTANTIALLY COMPLETE CONTAINMENT

2.1 INTRODUCTION

The ambiguity in the regulatory requirement in 10 CFR 60.113 for "Substantially Complete Containment" has resulted in the exploration of ways to quantify the requirement. Three reports were produced by the CNWRA that dealt with the feasibility of a quantitative demonstration of "substantially complete containment". The first of these reports listed the technical considerations necessary for evaluating "substantially complete containment", but did not address approaches to quantitative prediction. The second report detailed the uncertainty evaluation methods for waste package performance assessment, but did not address any specific information to which these uncertainty analysis methods will be applied. The third report delineated the various alternatives for quantitatively clarifying the concept of "substantially complete containment" in the current regulation. The main objective of this task is to demonstrate the feasibility of a quantitative assessment of substantially complete containment through an example analysis.

Quantitative assessment of substantially complete containment involves two activities: (i) the selection of failure modes and the development/modification of models that will be used in the example analysis, and (ii) coding and performing the example analysis. For the purposes of the example analysis, the loss of containment is defined as the through-wall penetration of a container by a defect. Although the analysis can be generalized for a variety of materials and Engineered Barrier System (EBS) designs, it is assumed here that the container is a thin-walled (6 mm thick) cylinder made of type 304L stainless steel designed according to the reference design presented in the U.S. Department of Energy (DOE) Site Characterization Plan (SCP) for Yucca Mountain. It is also assumed that the waste package boundary is the container boundary. It is anticipated that the example analysis will yield both a set of deterministic measures and a methodology for obtaining a family of Complementary Cumulative Distribution Functions (CCDF) in the form of the probability of having N or more breached containers in t years.

The objective of this report is to describe the type of models required to assess the performance of the container and the justification for the choice of specific approaches. A secondary objective is to point out the type of experimental data necessary to demonstrate adequacy of container designs.

2.2 INITIAL ASSUMPTIONS

In selecting appropriate models for the example analysis, the following general assumptions have been made:

- The container surface is exposed to an aqueous environment, at least for some containers. This is a departure from the intended design (Farmer et al., 1991) where the surface temperature of the containers was assumed to be above the unconstrained boiling point of water for over 1000 years. However, the assumption of aqueous environment contacting the container is justifiable for the following reasons: (i) It represents an extreme case. The corrosion rate in the vapor/steam phase is negligible (Farmer et al., 1991), and, hence, the temporal origin of failure events can be shifted to the time at which liquid water contacts the containers. Although stress corrosion cracking has been observed in the vapor phase, some

of these observations are related to the presence of a thin condensate film; (ii) The gravity-driven back flow of water through a fracture intersecting the borehole has been suggested by a number of investigators (Pruess et al., 1990; Buscheck et al., 1992); and (iii) Back flow of water has been observed in a number of field heater experiments (Zimmerman et al., 1986; Patrick, 1986; Ramirez et al., 1991). The effect of alternating wet and dry environment is taken into consideration in terms of the changes in the concentration of various ionic species in the aqueous environment contacting the container.

- Spatial variability in the corrosion and critical potentials throughout the surface of any given container is ignored. This is not a realistic assumption given the metallurgical inhomogeneities and the environmental variations within a borehole. However, this is used as a simplifying assumption in the example problem.

- The contribution of components of the EBS other than the outer container, is not considered. It is expected that the stainless steel canister (in the case of glass waste), Zircaloy fuel cladding, and any buffer/backfill may provide added containment.

- The effects of welding are not explicitly calculated, although the stresses for mechanical failure are assumed to be from residual stresses in terms of a certain fraction of the yield stress. This is partly because a reference welding process has not been chosen although a list of preferred welding processes has been identified (Robitz et al., 1992). Further, many of the factors affecting the performance of weldments such as residual stresses and heat-affected-zone (HAZ) microstructure are critically dependent on welding process, joint design, and fixturing. Finally, the effect of welding on localized corrosion behavior can be, as a first approximation, considered in terms of an empirical correction term to the behavior of the base metal.

2.3 OVERALL APPROACH

All the aqueous corrosion processes are dependent on the corrosion potential of the metal exposed to a particular environment under consideration. The modeling of corrosion potential is considered to be the backbone of the performance assessment of metallic containers (Walton and Sagar, 1988; Macdonald and Urquidi-Macdonald, 1990; Marsh et al., 1987). The corrosion potential is defined as the potential at which the current due to all the cathodic processes is equal to the current due to all the anodic processes including the electrochemical dissolution of the metal.

$$\sum_{j=1}^{n} I_{aj} - \sum_{j=1}^{n} I_{cj} = 0 \qquad (2\text{-}1)$$

where I_{aj} refer to the anodic (oxidation) currents including that of the metal dissolution (called the corrosion current, I_{corr}) and I_{cj} refer to the cathodic (reduction) currents. The corrosion potential of a given metal will vary with time depending on a number of factors such as temperature, environment composition, radiolysis, transport processes near the metal-environment interface, and photoelectrochemical processes in the passive film. Ideally, once the corrosion potential is known at any time, the initiation, propagation, or repassivation (cessation) of various corrosion processes can be determined by comparing the corrosion potential to the "critical potential" for those processes. For

example, most pitting models, be they stochastic or deterministic, assume that pitting is initiated on a freely corroding metal once the corrosion potential exceeds a critical potential. Similarly, a critical potential for initiation of crevice corrosion can be identified. In reality, however, the response of the metal is more complex because the time for initiation or repassivation is potential dependent. For the present analysis, the initiation and repassivation times are ignored, and the lowest potentials for initiation or repassivation are used. The case of stress corrosion cracking is more complex, but regions of potential where stress corrosion cracking can occur have been identified in many alloy-environment systems (Staehle, 1990).

The general approach to predicting the performance of a single container or a set of "identical" containers is illustrated in Figure 2-1, where pitting is considered to be the only failure mechanism. The corrosion potential initially increases, perhaps driven by radiolytic generation of oxidizing species such as H_2O_2. However, the increase in temperature in the initial period has an opposing influence because of decreased solubility of oxygen and increased decomposition or recombination of radiolytically generated species. The corrosion potential finally decreases to a value dictated by the diffusion limited reduction of oxygen at the metal surface. In addition to the cathodic processes, changes in anodic reaction kinetics, such as a decrease in passive current density due to film aging, can influence the corrosion potential. There can also be other processes influencing the variation of corrosion potential including the presence of active pits or crevice sites and incidental galvanic contact with carbon-steel borehole liner. For the case of failure by pitting, there is a distribution of pit initiation potentials even for a single container which is dictated by factors such as inclusion distribution (Stewart and Williams, 1992). As shown in Figure 2-1, after time t_1, pits begin to initiate for the container under consideration and grow. After time period t_2, the corrosion potential is below the pitting potentials, and, hence, no new pits initiate. The pits that have already been initiated at times t_1 through t_2, continue growing till the corrosion potential drops below the repassivation potential at time t_3. After this time period, the pits will cease to grow. Hence, the performance of this container in terms of its resistance to pitting penetration is dictated by the maximum depth of pits grown in the time period between t_1 and t_3. If this maximum depth is equal to the thickness of the container, the containment is considered to be lost. The methodology described above, when carried out for a number of containers, is similar to the damage function approach proposed by Macdonald and Urquidi-Macdonald (1992).

In the following sections, models for predicting corrosion potential of a container material will be reviewed. Empirically developed equations for critical potentials will be reviewed for use in failure time calculations. The need to develop more detailed models for justifying the use of these empirical equations will be discussed.

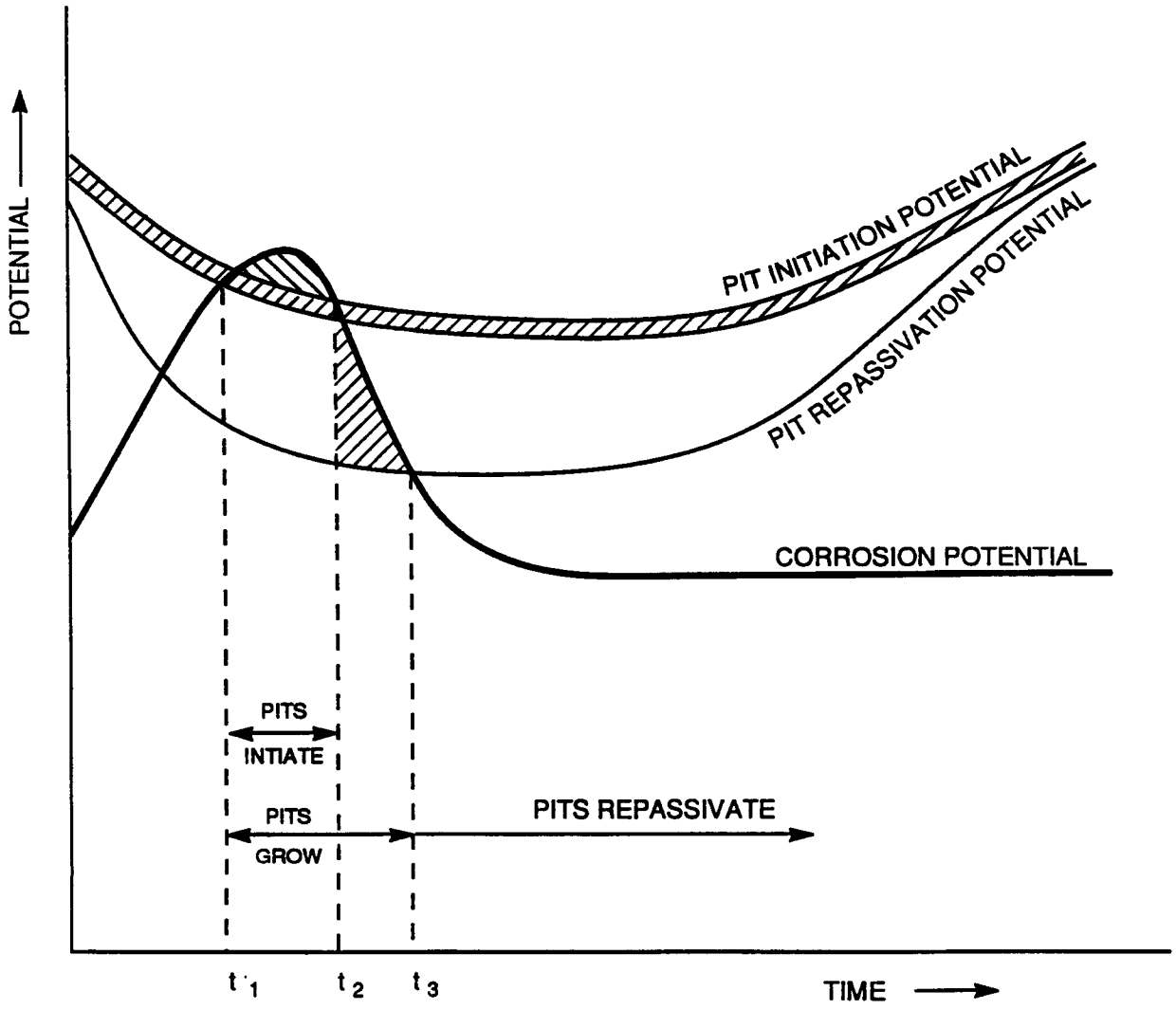

Figure 2-1. Schematic illustration of the use of corrosion, pitting, and repassivation potential to predict the performance of a container

3 CORROSION POTENTIAL MODELS

3.1 PRESENT MODELS

Calculation of the corrosion potential as a function of time has been made by Walton and Sagar (1988) for carbon-steel in a saturated environment for the Basalt Waste Isolation Project (BWIP). Calculation of the corrosion potentials for a variety of austenitic stainless steels and Cu-base alloys in an unsaturated environment for the Yucca Mountain repository site was made by Macdonald and Urquidi-Macdonald (1990). The approaches used in both these models are essentially the same with differences introduced by the differences in the materials and environments.

As mentioned in the previous section, the corrosion potential is the potential at which the net current due to anodic and cathodic processes is zero (Eq. 2-1). The dependence of the anodic and cathodic current densities on potential is determined by the rate determining step of the overall process. If the rate controlling process is charge transfer on an active, unfilmed surface, then the net current density on the metal is given by a Butler-Volmer type equation (Vetter, 1967):

$$i_j = i_{0j}\left[\exp\left(\frac{\alpha_j F}{RT}\eta_j\right) - \exp\left(-\frac{(1-\alpha_j)F}{RT}\eta_j\right)\right] \tag{3-1}$$

where,

i_{oj} is the exchange current density for the j^{th} reaction
$\eta_j = E_j - E_{eqj}$ is the overpotential
F is the Faraday constant
α_j is the charge transfer coefficient
R is the gas constant
T is the temperature in °K.

The exchange current density is given by:

$$i_{0j} = k_{+j}\, C_{rj} \exp\left(\frac{\alpha_j F}{RT}E_{eqj}\right) = k_{-j}\, C_{oj} \exp\left(-\frac{(1-\alpha_j)F}{RT}E_{eqj}\right) \tag{3-2}$$

where k_{+j} and k_{-j} refer to the anodic (oxidation) and cathodic (reduction) reaction rate constants, respectively, and C_{rj} and C_{oj} are concentrations of reduced and oxidized species, respectively. E_{eqj} is the equilibrium potential for a given partial electrochemical reaction given by the Nernst equation:

$$E_{eqj} = E_{0j} + \frac{RT}{nF}\sum \nu_i \ln a_i \tag{3-3}$$

where E_{oj} is the standard potential (equilibrium potential where the reaction species are in their standard states) and ν_i is positive for oxidized species and negative for the reduced species. It must be noted that the reaction rate constants in Eq. 3-3 are dependent on the assumed reference potential (Vetter, 1967). Typically, the values of exchange current density are used directly from experimental measurements without recourse to Eq. 3-3. It must be emphasized that the Eq. 3-1 is strictly valid only when charge transfer process is the rate determining step. It does not consider transport process as the rate

determining step. At potentials sufficiently cathodic to the equilibrium potential, $|\eta| \gg RT/zF$, and the first term in Eq. 3-1 vanishes (η is negative) and Eq. 3-2 has the form of a Tafel relationship ($\eta = a - b \log i$).

At the other extreme in many electrochemical corrosion processes, is the case where transport of reacting species to or away from the electrode (container) surface is the rate determining step. In a pure diffusion limited case, the current density corresponding to the partial reaction is controlled by diffusion. In a sense, this represents an equilibrium situation because the charge transfer processes are assumed to be sufficiently fast to have attained equilibrium (Vetter, 1967). In other words, Nernst equation (Eq. 3-3) can be used to calculate the potential with an important difference: the surface concentration of species (outside the diffuse double layer) involved in the calculation of potential is determined by the diffusion current density. If the surface concentrations of species are termed c_j, and the equilibrium (bulk) concentrations are C^o_j, the overpotential due to purely diffusion controlled process is given by (Vetter, 1967):

$$E_{diff} - E_{eq} = \frac{RT}{nF} \sum \nu_j \ln\left(\frac{c_j}{C_j^0}\right) \tag{3-4}$$

Where ν_j are the stoichiometric coefficients and n is the net electron transfer. The concentrations are used instead of activities for simplicity. The concentrations c_j at the metal-electrolyte interface are determined by transport given by (Walton and Sagar, 1988):

$$\gamma R_d \frac{dc_j}{dt} = \nabla\left[\gamma D \nabla c_j + \gamma D_M \nabla c_j - \nu c_j\right] + R_i \tag{3-5}$$

where

R_d	=	Retardation factor
c_j	=	Concentration of species
D	=	Coefficient of hydrodynamic dispersion
D_M	=	Molecular diffusion coefficient
ν	=	Darcy velocity
γ	=	Porosity
R_i	=	Reaction terms including radiolysis

The overall polarization behavior of a cathodic process such as oxygen reduction is illustrated schematically in Figure 3-2. As the electrode is polarized away from the equilibrium potential, the current-voltage relationship is represented initially by Eq. 3-1 (charge transfer process). However, at high polarization potentials, the current density assumes a limiting value dictated by transport and reaction controlled processes (Eq. 3-4). The overall current-potential relationship for any of the cathodic process can then be represented as (Vetter, 1967):

$$i = i_0\left[\frac{c_r}{C_r^0}\exp\left(\frac{\alpha z F}{RT}\eta\right) - \frac{c_o}{C_0^0}\exp\left(-\frac{(1-\alpha)zF}{RT}\eta\right)\right] \tag{3-6}$$

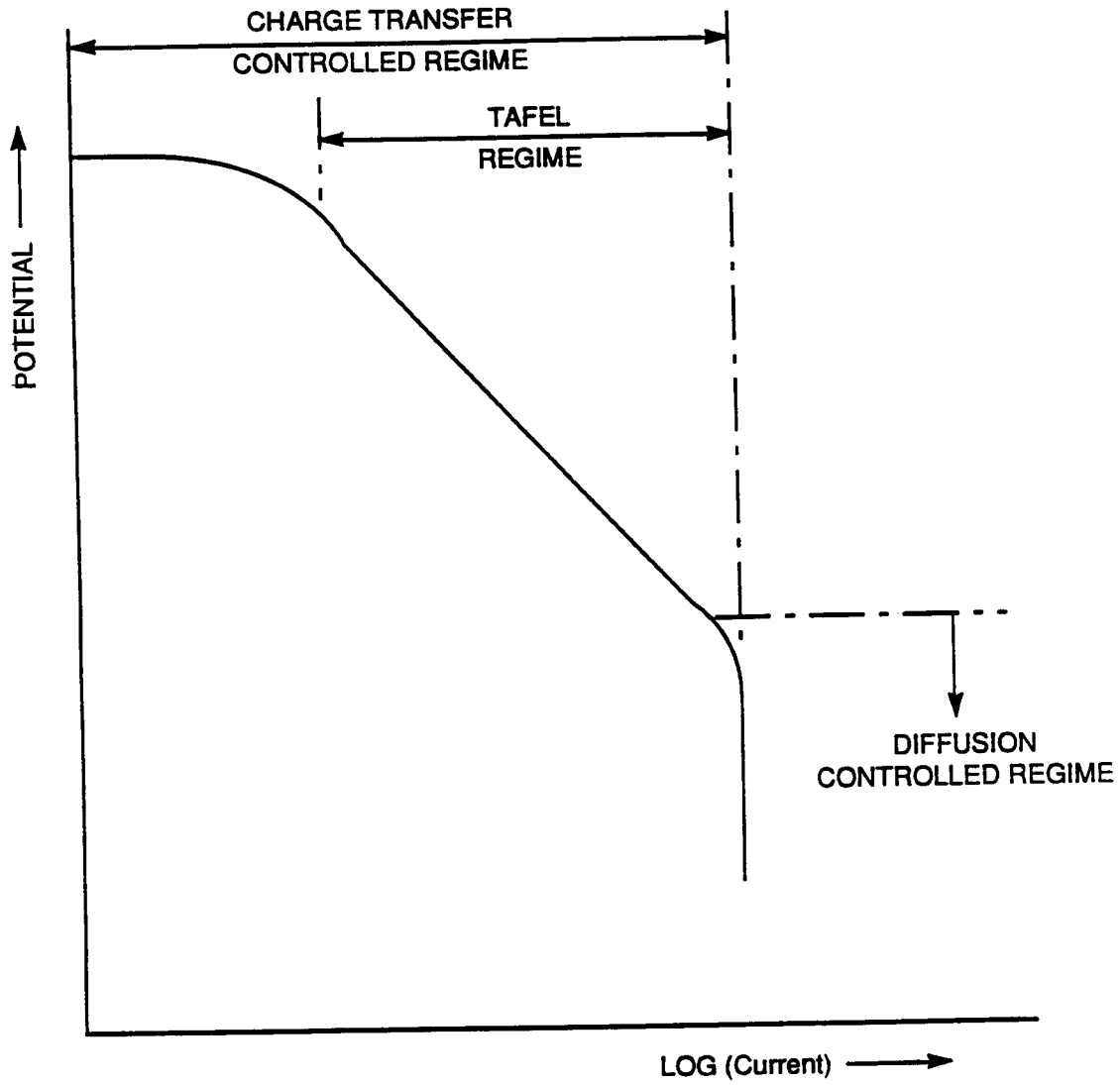

Figure 3-1. Schematic illustration of a cathodic polarization curve indicating charge transfer (activation) polarization, Tafel regime, and transport/reaction polarization

where c_r and c_o are the surface concentrations of reduced and oxidized species, respectively, and C_r^o and C_o^o are the equilibrium (bulk) concentrations. The surface concentrations are determined by Eq. 3-5. This is somewhat different from the approach used by Macdonald and Urquidi-Macdonald (1990) where a strictly charge-transfer controlled process was assumed to calculate the redox potential.

In order to calculate the corrosion potential, the anodic polarization behavior of the container metal is needed. It is difficult to represent the total active-passive-transpassive behavior of a metal mathematically, and, hence, it is generally assumed that the sum of the relevant cathodic reactions intersect the anodic polarization curve of the metal either in the active or the passive regime (Walton and Sagar, 1988). In the passive regime (Fig. 3-3), the anodic current is essentially potential independent, given by the passive current, I_p. In such a simplified case, the corrosion potential can be calculated by summing all the cathodic currents to equal I_p and using this value in Eq. 3-6.

3.2 LIMITATIONS OF THE PRESENT MODELS

The major limitation of the present models is the lack of availability of kinetic parameters for the various cathodic reactions. Macdonald and Urquidi-Macdonald (1990), while acknowledging uncertainties, were forced to use values of exchange current density on the basis of a general classification into slow, fast, and intermediate reactions. However, these values are extremely sensitive to the substrate and solution compositions. For example, the exchange current density used for oxygen reduction reaction was 10^{-12} A/cm^2. In a review of the oxygen electrode, Will (1976) suggests that the exchange current density can range from 10^{-22} A/cm^2 for gold to 10^{-5} A/cm^2 for palladium. Similar uncertainties accompany the other important reduction reaction, that of H_2O_2. The tremendous dependence of the kinetics of these reduction reactions on substrate can be seen in the effect of these oxidized species on the corrosion potentials of Pt and alloy 825 (Sridhar, Cragnolino, and Machowski, 1990). Aeration increased the corrosion potential of alloy 825 by 247 mV whereas it increased that of Pt by 648 mV. In contrast, the addition of H_2O_2 increased the corrosion potential of alloy 825 by 663 mV, but that of Pt by 557 mV. The catalytic decomposition of H_2O_2 on Pt and transition metals is also a factor in the overall reduction kinetics.

Another limitation is the lack of systematic data on the change in the passive current density with time of exposure. In particular, Macdonald and Urquidi-Macdonald (1990) calculate the time-average passive current density of all the alloys from the weight-loss data in long-term exposure tests. Firstly, this is not mechanistically justified for copper based alloys because, under some environmental conditions relevant to the Yucca Mountain repository site, they exhibit active behavior. Secondly, it does not take into consideration the changes in the electronic properties of the film as a function of time. For example, Gorse, Joud, and Baroux (1992) showed that aging the film under dry conditions can produce significant changes in the corrosion and pitting potentials of stainless steels.

A third limitation, particularly of the Macdonald and Urquidi-Macdonald (1990) model, is the assumption that a thin film of aqueous phase is present even at temperatures of 250°C. It is more likely that the temperature of those containers which are exposed to an aqueous environment will remain close to the boiling point of water. Thus, the variation in temperature, at least during the initial period of intense radioactivity, may not be an important factor for these containers.

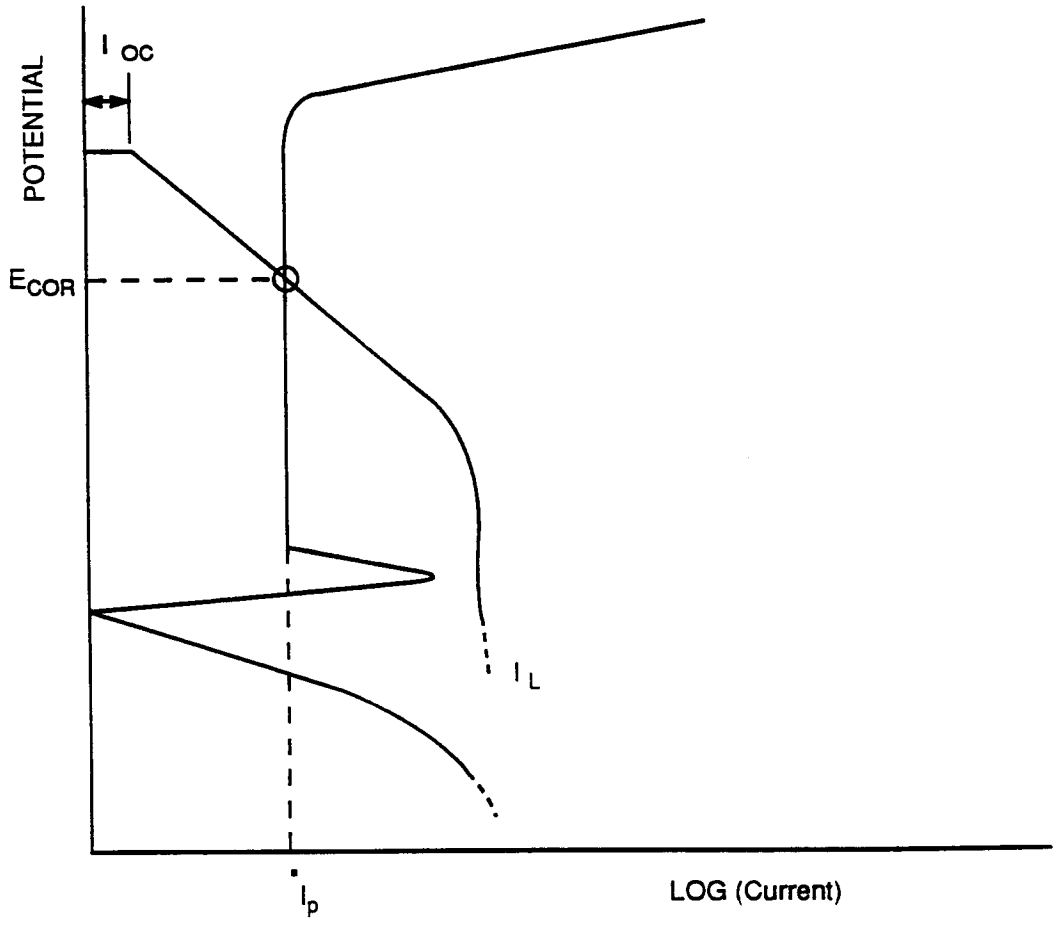

Figure 3-2. Schematic diagram illustrating the concept of a corrosion potential for an active-passive alloy. Both the anodic and cathodic curves are represented on the same side of the axis for convenience. I_L is the limiting current. I_{oc} is the exchange current for the cathodic reaction

3.3 RECOMMENDED APPROACH

As observed in the preceding paragraphs, the model for obtaining the corrosion potential as a function of time is relatively well established. However, there is much uncertainty in the input parameters. Hence, one of the important tasks of the "substantially complete containment" example analysis will be to evaluate the changes in the predicted corrosion potentials to changes in input parameters such as exchange current density, passive current density, temperature, and concentration of radiolytic species. This will be done initially as a parametric study and a more complete uncertainty analysis will be explored later. For this purpose, it is recommended that a simplified version of the Macdonald and Urquidi-Macdonald model be considered where only the most oxidizing radiolytic species with high values of yield G, are considered. This may include H_2O_2, OH, and HO_2. Species, such as H and e^-_{aq}, need not be considered because of their highly negative standard potentials, and oxidizing species, such as O_2^-, need not be considered because of their low radiolytic yield (Macdonald and Urquidi-Macdonald, 1990).

4 PITTING MODELS

4.1 PRESENT MODELS

4.1.1 Pit Initiation

A more detailed review of the available models for pitting corrosion is being performed as part of the Engineered Barrier System Performance Assessment (EBSPAC) development program. Because of the need to balance rigor of the models with the speed of computation, simple parametric equations will be used in the "Substantially Complete Containment" example analysis and more detailed auxiliary models will be developed in the EBSPAC program. As shown in Figure 2-1, pitting can be divided into initiation, growth, and repassivation steps. The fundamental mechanisms of pit initiation and repassivation are still under debate with many mechanistic interpretations being able to account for at least some of the pitting phenomena. More recently, the stochastic nature of pit initiation process has been recognized and quantified (Shibata and Takeyama, 1977; Henshall, 1992; Williams, Westcott and Fleischmann, 1985). These models suggest that stable pits are preceded by unstable pitting events where pits are continually generated and repassivated. However, even the stochastic models invoke a minimum critical potential below which neither unstable nor stable pits nucleate. Hence, a mechanistic model is needed to provide a fundamental justification for a critical pitting potential. For the example analysis, the experimental data on pit initiation potential of type 304/304L stainless steel will be examined for the most appropriate values.

Experimental investigations on type 304 stainless steel (Wang, Su, and Smialowska, 1988) in aerated chloride solutions at temperatures ranging from 25 to 200°C have shown that the pit initiation potential is dependent on both the chloride concentration and temperature as shown below.

$$E_p = A - B\log[Cl^-] \tag{4-1}$$

where B was 0.15V/decade for temperatures up to 80°C and 0.1 V/decade for temperatures from 80 to 200°C. This is in general agreement with many other experimental data (Szklarska-Smialowska, 1986). More recent results at temperatures ranging from 100 to 150°C (Yashiro and Tanno, 1992) have shown the relationship in Eq. 4-1 to be true even when activity coefficient changes with temperature and chloride concentrations are taken into account. The value of A in Eq. 4-1 decreases with an increase in temperature for many materials, but its functional dependence varies for different alloy systems (Szklarska-Smialowska, 1986). For type 304/304L stainless steels, the value of A decreases linearly with temperatures in the range of 30 to 95°C. However, some investigators have also found that pitting potential for type 304 stainless steel increases linearly with 1/T, where T is in °K (Szklarska-Smialowska, 1986). For simplicity, a linear dependance of A with temperature will be assumed in the example analysis. Results in the literature also show that the E_p is independent of pH over a wide range of pH values up to a pH of 10. These results are in agreement with more recent results generated at the CNWRA.

4.1.2 Pit Repassivation

The effect of environmental factors on repassivation potential of type 304/304L stainless steel has not been as widely investigated. Yashiro and Tanno (1990) investigated the repassivation potential for pitting of type 304 stainless steel in NaCl at temperatures ranging from 150 to 250°C. They found

that the repassivation potential also showed a logarithmic relationship similar to Eq. 4-1. However, the slope B was smaller by a factor of 4 than that for pit initiation potential. This is understandable if one realizes that the chloride concentration inside a growing pit is much higher than the bulk chloride concentration. They also found that the value of A in Eq. 4-1 for repassivation potential decreased with an increase in temperature. Repassivation potentials were independent of pH for a pH range of 2 to 13. This type of relationship is in qualitative agreement with more recent investigations conducted at lower temperatures at the CNWRA.

4.1.3 Pit Growth

Böhni and Hunkeler (1990) reviewed the growth kinetics of pits on a variety of alloy systems including austenitic stainless steels. Essentially, three regimes of pit/crevice corrosion growth can be delineated: (i) diffusion controlled regime, (ii) charge-transfer controlled regime, and (iii) ohmic potential drop controlled regime. In the case of austenitic stainless steels, it has been shown that a salt film of metal chlorides ($FeCl_2$ and $NiCl_2$) precipitates on the walls of an actively growing pit at relatively moderate applied potentials (200 mV vs. SCE), and the growth of the pits is then controlled by the diffusion of these highly soluble species away from the pit bottom. Under these conditions, it has been shown that the pit depth, d_p, is given by

$$d_p = -\delta^0 + \left[(\delta^0)^2 + \frac{2zFD\Delta C}{c}t\right]^{\frac{1}{2}} \qquad (4\text{-}2)$$

where δ^0 is a correction factor for effective diffusion path, ΔC is the concentration difference of the diffusing metal ion between the pit bottom and the bulk, D the diffusion coefficient of the metal chloride species under consideration, and c a conversion factor for units (Böhni and Hunkeler, 1990). The concentration inside pits corresponds to the solubility limit for $FeCl_2$ in the case of type 304 austenitic stainless steel. From Eq. 4-2, it can be seen that the pit growth rate is independent of applied potential in the diffusion controlled regimes. The pit growth velocity in this regime is approximately 10^{-2} mm/minute, which is indeed quite large. At lower applied potentials, a semi-logarithmic dependence of growth velocity on potential was found, indicating a charge transfer controlled regime. For the case of type 304 stainless steel, the pit growth velocity decreased by two decades for a 200 mV decrease in applied potential. It can also be seen from Eq. 4-2 that once a diffusion controlled pit growth is established, the growth rate increases as the bulk metal ion concentration decreases because ΔC increases. In situations where there is significant stirring of the solution, pit growth rate is controlled by the ohmic potential drop in the solution. In this case, pit growth rate decreases as the bulk chloride concentration decreases due to the increase in solution resistivity.

From the foregoing discussions, it can be seen that stable pit growth has a maximum velocity corresponding to a diffusion controlled limit of about 10^{-2} mm/minute. For the example problem, this type of growth will be assumed. However, the experimental investigations that are underway in the Integrated Waste Package Experiments Program (IWPE) will provide input into the pit growth kinetics appropriate to the environmental conditions expected in the repository.

4.2 LIMITATIONS OF THE PRESENT MODELS FOR PITTING

The main limitation of the present models is the lack of a mechanistic model that can account for all the observed environmental effects on pitting. The mechanistic models also require many parameters that are difficult to measure. The stochastic models, while successful in explaining the distributed nature of pit initiation parameters, depend on a critical pit initiation potential as the lowest value of the potential below which no pits nucleate. Again a fundamental mechanistic explanation must be provided for this critical pit initiation potential. In the case of repassivation potential, there is still a controversy as to the existence of a unique repassivation potential for pitting. However, empirical evidence of a repassivation potential independent of prior pit growth exists and can be used for the example analysis. A detailed examination of mechanistic models addressing the issue of critical pitting potential will be conducted in the EBSPAC program in FY93.

5 CREVICE CORROSION

5.1 CREVICE CORROSION MODELS

5.1.1 Initiation and Repassivation

Detailed models of crevice corrosion initiation have been developed elsewhere in the program and by many investigators in the literature (Walton, 1992; Sridhar et al., 1990; Sharland 1991; Tsujikawa et al., 1987, Ahn, 1984). However, these models are difficult to incorporate in bigger codes because of their need for long computational time, although the models can be used for auxiliary analysis. One of the main limitations of all the crevice corrosion initiation models developed in the literature is that they cannot explain the observed critical potential for crevice corrosion initiation. A critical potential for crevice corrosion initiation, albeit in short term tests, has been observed, notably by Tsujikakwa and his colleagues (Tsujikakwa and Hisamatsu, 1984; Tsujikawa and Okayama, 1990). Tsujikawa and Hisamatsu (1984) established that a crevice initiation potential exists below which no crevice corrosion was found to occur up to about 15 hours of testing. This potential was dependent on chloride concentration and crevice geometry. A logarithmic dependence on chloride concentration similar to Eq. 4-1 was found where the slope was about 0.1 V/decade for type 316 stainless steel at 80°C. They also found that the repassivation potential for crevice corrosion, under slow scan rate testing (0.017 mV/sec) coincided with the critical crevice corrosion initiation potential. The effect of crevice geometry on repassivation potential was found in terms of the effect of crevice forming materials. The torque used to tighten the crevice surfaces together was not found to have a significant effect. This is probably because the soft crevice forming materials, such as asbestos, conformed to the surface profile of the metal, while the hard crevice forming material flattened the surface profile.

Tsujikawa and Okayama (1990) measured the crevice repassivation potential of a number of materials in various concentrations of chloride at temperatures ranging from 25 to 80°C. Yashiro et al., (1990) investigated the crevice corrosion initiation and repassivation of type 304 stainless steel in 0.5 M NaCl at temperatures ranging from 25° to 250°C. They showed that the repassivation potential for crevice corrosion is lower than the initiation potential for crevice corrosion. Additionally, they showed that the repassivation potential for crevice corrosion was lower than that for pitting up to a temperature of 150°C, above which they coincided. Below 150°C, the repassivation potential for crevice corrosion in the 0.5 M NaCl solution was given by

$$E_{rcrev}\ (mV\ vs.\ SHE\ at\ Temp.) = 1268 - 3.21T \qquad (5\text{-}1)$$

where T is in °K. Yashiro, Koshiyama, and Tanno (1991) also investigated the dependence of crevice repassivation potential of type 304 stainless steel in various chloride concentrations at 423°K and found a semi-logarithmic dependence on chloride concentration similar to Eq. 4-1 with a slope of 0.1 V per decade. However, the crevice repassivation potential, thus measured, was not a conservative figure since it depended on the extent of prior crevice corrosion.

5.1.2 Growth

The crevice corrosion growth models are not fundamentally different from pit growth models. However, there are significant differences in the geometry of crevices compared to pits. Unfortunately, modeling efforts have not focused as much on crevice corrosion growth as on initiation. In the absence of detailed models, the growth rate of crevices will be assumed to be the same as that of pits in terms of current density. The current density will be converted to a uniform corrosion rate of the crevice walls. However, it must be noted that this position is not defensible rigorously. For example, the polarization behavior of an actively corroding crevice can vary tremendously from the mouth to the bottom of the crevice. Secondly, in a deep crevice that is actively growing, the potential drop due to solution resistance will be significant so that the deepest part of the crevice may not be corroding at the same velocity as the mouth of the crevice. Finally, crevice corrosion growth can occur as pits inside the crevice rather than uniform wall thinning as shown by Yoshiro, Koshiyama, and Tanno (1991).

5.2 LIMITATIONS OF CURRENT MODELS

As can be seen from the above discussion, a number of empirical evidence for a critical crevice initiation and repassivation potential has been found. For long-term exposures, the current experimental data suggest that a lower-bound crevice repassivation potential will be sufficient to predict both initiation and repassivation. A limitation of most of the current models of crevice corrosion is that they cannot predict a critical potential for crevice corrosion initiation of austenitic stainless steels. The model proposed by Tsujikawa et al., (1987) for crevice corrosion repassivation cannot be readily used to predict the repassivation potential as a function of external solution chemistry or crevice geometry. Hence, further model development is needed to understand the repassivation of actively growing crevice corrosion.

6 STRESS CORROSION CRACKING

6.1 STRESS CORROSION CRACKING MODELS AND APPROACHES

Stress corrosion cracking (SCC) is a phenomenon by which ductile metals and alloys fail in a brittle manner through the initiation and propagation of cracks resulting from the combined action of a sustained tensile stress (applied and/or residual) and a specific corrosive environment. For High-Level Waste (HLW) containers, the environments of interest are aqueous, and they can be condensed layers of moisture or bulk solutions, both derived from groundwater compositions typical of the vadose zone. The alloy of interest in this particular example is type 304L stainless steel, which is known to be susceptible to SCC in chloride-containing solutions. Chloride is the main detrimental species present in groundwater. Although the SCC of austenitic stainless steel in chloride environments has been extensively studied and several SCC mechanisms have been postulated, no agreement exists in the literature regarding the mechanisms, despite a relatively good phenomenological understanding. This statement is valid for both the initiation and the propagation stage. A detailed review of different mechanisms, and the corresponding mathematical models where available, is being done as part of the development work in EBSPAC. What follows is a brief discussion of the important issues regarding SCC of HLW containers and the technical approach that will be adopted in the example problem.

Crack propagation, assuming the pre-existence of cracks and the validity of linear elastic fracture mechanics (LEFM), is not valid as a criterion for predicting the performance of HLW containers. At the lowest crack growth rate that can be measured in a reasonable test period with the existing technology (i.e., 2×10^{-12} m/s), a thin-wall container will be penetrated by a through-wall crack in approximately 200 years. This means that, unless a plausible mechanism for crack arrest can be postulated, the valid criterion for eliminating SCC failure of containers should be based on avoiding crack initiation. As discussed recently (Cragnolino and Sridhar, 1992), SCC of austenitic stainless steel, particularly types 304/304L and 316/316L SS, in chloride-containing solutions at temperatures higher than 80°C only occurs at potentials above a critical potential (E_{scc}). It appears (Tamaki et al., 1990) that E_{scc} in neutral chloride solutions corresponds to the repassivation potential for crevice corrosion (E_{rcrev}). As known, this potential increases with decreasing chloride concentration and with decreasing temperature. SCC initiation and propagation will occur if the corrosion potential of the alloy in the repository environment (E_c) is higher than E_{scc} as determined under the same environmental conditions. As an initial approximation, it will be assumed in this example that E_{scc} is equal to E_{rcrev} in a chloride-containing solution simulating the near-field repository environment.

Contrary to the case of pitting and crevice corrosion, the existence of a second characteristic potential, equivalent to the repassivation potentials defined for both localized corrosion phenomena, has not been demonstrated for SCC. In some particular cases, however, crack growth of an actively growing crack has been arrested by decreasing the corrosion potential or the applied potential to values just below E_{scc}. This effect of potential has been observed for the intergranular SCC of sensitized type 304 SS in high temperature (>250°C) aqueous solutions (Cragnolino, 1985; Indig, 1986), and probably is valid also for the transgranular SCC of the same alloy in chloride-containing solutions.

The approach to be adopted in the example analysis will be to assume that the initiation and the arrest of a propagating crack is controlled by the difference between E_{scc} and E_c for the same environment. At corrosion potentials above E_{scc}, an appropriate mathematical model for calculating crack growth rate will be used. One of the available models is that developed by Ford and Andresen (1985,

1988). Based on the film rupture, slip dissolution, and repassivation concepts the crack propagation rate expressed as follows:

$$da/dt = M\, Q_f\, \dot{\epsilon}_{ct} / z\, \rho\, F\, \epsilon_f \qquad (6\text{-}1)$$

where M and ρ are the atomic weight and density for the alloy respectively, F is the Faraday constant, z is the number of electrons involved in the oxidation of the alloy, ϵ_f is the fracture strain of the oxide, $\dot{\epsilon}_{ct}$ is the strain rate at the crack tip, and Q_f is the oxidation charge density. Equation (6-1) can be restated in a general form

$$da/dt = f(n)\ (\dot{\epsilon}_{ct})^n \qquad (6\text{-}2)$$

where the parameter n represents the effect of the environment and the alloy composition on the crack propagation rate and $f(n)$ is a coefficient which is a function of n. Under constant loading conditions $\dot{\epsilon}_{ct}$ is proportional to K^4, where K is the stress intensity factor.

This model is currently available as a code, PLEDGE, developed with the sponsorship of Electric Power Research Institute (EPRI) for the environmental, mechanical, and material conditions prevailing in recirculating lines of boiling water reactors. If arrangements can be made to have this code available, the possibility of extrapolating parameters and variables to the repository conditions will be evaluated to obtain at least approximate expressions of crack growth rate as a function of temperature and potential, even though other environmental variables, such as the effect of solution composition, cannot be properly considered with the existing database.

6.2 LIMITATIONS OF THE PRESENT MODELS

The existing models have many limitations for the proposed analysis. The Ford-Andresen model, for example, was developed for very low conductivity water at temperatures around 290°C to deal specifically with the intergranular SCC of sensitized type 304 SS on the basis of a relatively extensive database. Its validity for a nonsensitized material in more concentrated solutions at lower temperatures, in which SCC is transgranular, could be questionable in the absence of a comparable database, especially when much lower crack growth rates and greater associated uncertainties can be expected. Extensive work within the context of EBSPAC is needed to adapt existing models to the environmental conditions of the near-field in a HLW repository, taking into consideration heat transfer, distribution of residual stresses, and the effect of temperature variation with time as the input variables of the SCC models.

7 MECHANICAL FAILURE

7.1 BUCKLING FAILURE

Buckling can be caused by the sudden collapse of the borehole plug or the borehole walls, and by dynamic loads caused by seismic activity. For a given design, a time dependent waste package failure criteria due to buckling can be developed. The buckling of waste packages is essentially a three-dimensional phenomenon. Very often, detailed three-dimensional finite-element analysis is required to obtain a failure loading (static and dynamic) envelope for a given design. There are, in the literature, several analytical expressions for the buckling of cylindrical and plate structures. These are primarily for static loads that are symmetrically loaded with respect to a simplified geometry. In this version of Source Term Code (*SOTEC*), the buckling loads are based on analytical expressions (Bazant and Cedoltin, 1991) with significant simplifying assumptions.

The waste package is assumed to be a long slender cylinder subject to axial and vertical symmetric loads. The cylinder is unconstrained in the radial direction. As a conservative assumption, the stiffening effect of the wasteform inside the cylinder is neglected. The additional stiffness due to end plates is also not considered. The material properties are assumed to be functions of temperature. Only static or quasi-static loads are considered.

The buckling equations are developed for general conditions for various thickness to radius ratios. The approach adopted here considers two aspects of cylinder buckling. In the first evaluation, the load safety factor and critical buckling load are determined for three loading conditions: uniform radial load, uniform axial load, and uniform radial and axial load. Based on the current design configuration, only elastic buckling needs to be considered. Thus, in the second evaluation, only the critical thickness in the elastic buckling criteria is calculated by using the corresponding initial buckling load and safety factor.

7.1.1 Case 1 Evaluation

For safety reasons, the load factor must be applied to the original critical buckling load in order to determine a conservative buckling criteria. In this version, three load factors are determined using the following empirical forms:

- Plastic Buckling

$$F = 1.5 \text{ for } (R/t) \leq 5 \tag{7-1}$$

- Elastic-Plastic Buckling

$$F = 1.5+1.5\left[\frac{(R/t)-5)}{(R/t)_e-5}\right] \text{ for } 5 \leq (R/t) \leq (R/t)_e \tag{7-2}$$

- Elastic Buckling

$$F = 3.0 \text{ for } (R/t) \geq (R/t)_e \tag{7-3}$$

$$(R/t)_e = \sqrt{\frac{E}{4(1-\nu^2)\sigma_{pl}}} \qquad (7\text{-}4)$$

where

F = load factor
t = wall thickness, 0.01 (original) m
R = radius, 0.33 (original) m
(R/t) = radius to thickness ratio
$(R/t)_e$ = minimum R/t for elastic buckling
σ_{pl} = proportional limit stress = 0.8 x yield stress, σ_y
σ_y = yield stress, MPa = 170 x [1-1x10^{-3} x (T-20)]
T = current temperature (°C)
E = elastic modulus, MPa = 182000 x [1-6x10^{-4}x(T-20)]
ν = Poisson's ratio = 0.25 x [1+4x10^{-4}x(T-20)]

The critical buckling loads under uniform radial, uniform axial, and uniform radial and axial external loads are calculated. Buckling formulas for long thin-walled cylinders under uniform radial external loads are derived by:

- Elastic Buckling

$$P_{cr} = \frac{E}{4(1-\nu^2)}\left[\frac{t}{R}\right]^3 \qquad (7\text{-}5)$$

- Elastic-Plastic Buckling

$$P'_{cr} = \frac{E_1}{4(1-\nu^2)}\left[\frac{t}{R}\right]^3 \qquad (7\text{-}6)$$

- Plastic Buckling

$$P''_{cr} = \frac{t}{R}\sigma_y \qquad (7\text{-}7)$$

where

P_{cr} = elastic buckling pressure, MPa
P'_{cr} = elastic-plastic buckling pressure, MPa
P''_{cr} = plastic buckling pressure, MPa

E_t = tangent modulus, MPa = 1600 x [1-6x10^{-4}xT-20)] x [1-3.9x10^{-4} x (σ-275)] (σ represents the current pressure and T represents temperature °C).

Buckling formulas for long, thin-walled cylinders under uniform axial external load (for elastic buckling only) are derived from:

$$P_{cr} = \frac{1}{\sqrt{3}} \frac{E}{\sqrt{1-\nu^2}} \frac{t}{R} \tag{7-8}$$

7.1.2 Case 2 Evaluation

As discussed earlier, the elastic buckling is considered more important because of the current design configuration. In the following, the critical thickness for elastic buckling criteria under different loading conditions is calculated. Assuming a uniform radial external load, P_E, and a safety factor of three, buckling occurs when

$$\frac{P_E}{3} \geq P_{cr} \geq \frac{E}{4(1-\nu^2)} \left[\frac{t}{R}\right]^3 \tag{7-9}$$

The critical thickness, t_c, can be

$$t_c = \frac{0.32(a)}{1-(a)} \tag{7-10}$$

where

$$a = \frac{4P_E(1-\nu^2)^{1/3}}{3E}$$

For a uniform axial external load in the elastic range with a safety factor of three, buckling occurs when

$$\frac{P_E}{3} \geq P_{cr} \geq \frac{1}{\sqrt{3}} \frac{E}{\sqrt{1-\nu^2}} \frac{t}{R} \tag{7-11}$$

The critical thickness is

$$t_c = \frac{0.32(a)}{1-(a)} \tag{7-12}$$

where

$$(a) = \frac{P_E\sqrt{(1-\nu^2)}}{\sqrt{3}E}$$

For a uniform axial and radial external load, buckling failure occurs when

$$\frac{P_E}{3} \geq P_{cr} \geq \frac{0.92E}{\left[\frac{L}{R}\right]\left[\frac{R}{t}\right]^{2.5}} \qquad (7\text{-}13)$$

where L is the length (height) of the container.

The critical thickness, t_c, can be derived by using numerical analysis. Failure due to buckling is assumed to occur when the calculated critical thickness is greater than the current (corroded) thickness or when the external load exceeds the critical buckling load.

7.2 OVERLOAD FAILURE

7.2.1 Linear Elastic Fracture Mechanics Approach

The overload failure can occur if the combination of net section stress and defect size exceeds a critical condition for fast fracture. In the case of cracks in an elastic field, the critical condition for fast fracture is usually calculated using LEFM in terms of a stress intensity factor, which under plane strain conditions, is termed K_{IC} or plane strain fracture toughness of the material. The stress intensity factor, K_I, is given by

$$K_I = Y\sigma(a)^{0.5} \qquad (7\text{-}14)$$

where a is the crack length, σ is the nominal stress, and Y is a geometric constant dependent on the loading and crack configurations. However, the plane strain fracture toughness provides a conservative lower limit criterion for fast fracture. For the containers, the stress field and defect size will be a function of time. In the example analysis, the stress field is assumed to originate mainly from the residual stresses due to circumferential closure welding. Thermal, lithostatic, and hydrostatic stresses are neglected.

7.2.2 Limitations of LEFM Approach

A limitation in using K_{IC} as a failure criterion is that, for type 304 stainless steel, it is quite high and the wall thickness is low so that the condition for plane strain condition implied in the use of K_{IC} will not be strictly valid. For example, the K_{IC} value for an annealed type 304 stainless steel is likely to be over 200 Ksi.√in., and its yield strength is about 40 Ksi. Based on these values, the minimum thickness for plane strain conditions to be valid is 62 inches! A second, more compelling, limitation of this approach is the assumption of long cracks which permits the use of a single parameter, K, to characterize the crack-tip stress field. This is valid if the crack length is approximately twenty times the plastic zone size. Since the crack length, a, cannot be greater than the container thickness, t, the maximum stress intensity factor below which LEFM can be used to predict container failure is given by

$$r_y \leq \frac{t}{20} = \frac{1}{2\pi}\left(\frac{K}{\sigma_y}\right)^2 \qquad (7\text{-}15)$$

where r_y is the plastic zone radius and σ_y is the yield strength. Using the yield strength for type 304L stainless steel of 40 Ksi and thickness of 0.5 inch, the maximum stress intensity for validity of LEFM is about 16 Ksi.$\sqrt{in}$. It can be seen that this low value of stress intensity factor can be met only under severe conditions of SCC corrosion fatigue. In future developments, elastic-plastic fracture mechanics approach will be considered to overcome some of the above described limitations

8 SUMMARY AND RECOMMENDATIONS

The approach and models that will be used in the example analysis of the feasibility of quantification of the term "Substantially Complete Containment" in 10 CFR60.113(a) are evaluated in this report. For the purpose of the example analysis, at least some of the containers will be assumed to come into contact with an aqueous environment. The corrosion rate for the containers that remain dry will be assumed to be negligible. The focus of the example analysis will be type 304/304L stainless steel. The basic approach will consist of modeling the corrosion potential of the container as a function of time and comparing this to critical potentials for initiation and repassivation of pits, crevices, and stress corrosion cracks. The models for corrosion potential were reviewed. A diffusion-charge transfer controlled corrosion potential model is recommended. Of the radiolysis reactions, only three involving oxidizing species may need to be considered for the initial model development. The formation of nitrogen species is not considered to be important in the initial stages of this model development as they are formed mainly in moist vapor environments. The limitations of the input parameters to the corrosion potential models were pointed out. Because of the uncertainties involved in the input parameters, it is recommended that sensitivity analysis of the corrosion potential model be conducted as the first step of the example analysis.

Models for pitting, crevice corrosion, and stress corrosion cracking were reviewed briefly. More detailed reviews of these models are part of the EBSPAC program that is ongoing. However, sufficient empirical data exists to formulate parametric equations of the critical pit initiation and repassivation potentials in terms of chloride concentration and temperature. The dependence on other environmental factors such as pH, sulfate, and nitrate are relatively minor, at least for type 304/304L stainless steel. The type of parametric relationship for crevice corrosion is the same as for pitting. For the case of stress corrosion cracking, not much empirical data is available to determine a critical potential for initiation of stress corrosion cracking. However, crevice corrosion repassivation potential will be used as the critical potential for stress corrosion cracking in the example analysis based on the experimental results of Tamaki et al., (1990). The limitations of the current models for all three corrosion processes and mechanical failure modes are pointed out.

9 REFERENCES

Ahn, T.M. 1984. *A Model for the Initiation of Crevice Corrosion in Grade-12 Titanium in a Brine Solution.* BNL-NUREG-34792. Upton, NY: Brookhaven National Laboratory (BNL).

Andresen, P.L. and F.P. Ford. 1985. Modeling and life prediction of stress corrosion cracking in sensitized stainless steel in high temperature water. *Predictive Capabilities in Environmentally Assisted Cracking*. R. Rungta, ed. New York, NY. The American Society of Mechanical Engineers (ASME): PVP-99: 17-38.

Bazant, Z.P. and L. Cedolin. 1991. *Stability of Structures.* New York, NY: Oxford University Press.

Böhni, H., and F. Hunkeler. 1990. Growth kinetics and stability of localized corrosion processes. H. Isaacs et al., eds., *Advances in Localized Corrosion.* Houston, TX: National Association of Corrosion Engineers (NACE): 69-74.

Buscheck, T.A. and J.J. Nitao. 1992. The impact of thermal loading on repository performance at Yucca Mountain. *High-Level Radioactive Waste Management. Proceedings of the Third International Conference.* La Grange Park, IL: American Nuclear Society (ANS): 1003-1017.

Cragnolino, G. 1985. The significance of a critical potential in the intergranular stress corrosion cracking of stainless steel piping in BWR environments. *Predictive Capabilities in Environmentally Assisted Cracking*. R. Rungta, ed. New York, NY: ASME: PVP-99: 293-318.

Cragnolino, G. and N. Sridhar. 1992. *A Review of Stress Corrosion Cracking of High-Level Nuclear Waste Container Materials - I.* CNWRA 92-02. San Antonio, TX: Center for Nuclear Waste Regulatory Analyses.

Farmer, J.C., G.E. Gidowski, R.D. McCright, and H.S. Ahluwalia. 1991. *Corrosion models for performance assessment of high-level radioactive waste containers*. Nuclear Engineering and Design 129: 57-88.

Ford, F.P. and P.L. Andresen. 1988. Development and use of a predictive model of crack propagation in 304/316L, A533B/A508 and Inconel 600/182 alloys in 288°C water. G.J. Theus and J.R. Weeks, eds. *Proc. Third International Symposium Environmental Degradation of Materials in Nuclear Power Systems-Water Reactors*. Warrendale, PA. The Metallurgical Society (TMS): 789-800

Gorse, D., J.C. Joud, and B. Baroux. 1992. The effect of ageing on passive films formed on stainless steels by annealing in hydrogen atmospheres. *Corrosion Science* 33(9):1455-1478.

Henshall, G.A. 1992. Stochastic models for predicting pitting corrosion damage of HLW containers. *Proceedings of the Topical Meeting on Nuclear Waste Packaging Focus '91.* La Grange Park, IL: ANS: 225-232.

Indig, M.E., B.M. Gordon, R.B. Davis, and J.E. Weber. 1986. Evaluation of in-reactor intergranular stress corrosion cracking via electrochemical measurements. *Proc. Second International Symposium Environmental Degradation of Materials in Nuclear Power Systems-Water Reactor.* La Grange Park, IL: ANS: 411-418.

Macdonald, D.D. and M. Urquidi-Macdonald. 1992. The corrosion damage function — interface between corrosion science and engineering. *Corrosion* 48 (5):354-367.

Macdonald, D.D. and M. Urquidi-Macdonald. 1990. Thin-layer mixed potential model for the corrosion of high-level waste canisters. *Corrosion* 46(5):380-390.

Marsh, G.P., K.J. Taylor, S.M. Sharland, and P.W. Tasker. 1987. An approach to evaluating the general and localized corrosion of carbon-steel containers for nuclear waste disposal. J.K. Bates and W.B. Seefeldt, eds. *Materials Research Symposium Proceeding V.84. Scientific Basis for Nuclear Waste Management X.* Pittsburgh, PA: Materials Research Society (MRS): 227-238.

Patrick, W.C. 1986. *Spent-Fuel Test - Climax: An Evaluation of The Technical Feasibility of Geologic Storage of Spent Nuclear Fuel in Granite.* UCRL-53720. Livermore, CA: Lawrence Livermore National Laboratory (LLNL).

Pruess, K., J.S.Y. Wang, and Y.W. Tsang. 1990. On thermohydrologic conditions near high-level nuclear wastes emplaced in partially saturated fractured tuff. I. Simulation studies with explicit consideration of fracture effects. *Water Resources Research* 26: 1235-1248.

Ramirez, A.L. 199 *Prototype Engineered Barrier System Field Test (PEBSFT) Final Report.* A.L. Ramirez ed., UCRL-ID-106159. Livermore, CA: LLNL.

Robitz, E.S., H.A. Damian, C.C. Conrady, R.L. Fish, E.W. Russell. 1992. Status report — fabrication and closure development of nuclear waste disposal containers for the Yucca Mountain project. *Proc. Nuclear Waste Packaging. Focus'92* La Grange Park, IL: ANS: 136-143.

Sagar, B., R.B. Codell, J.Walton, and R.W. Janetzke. 1992. SOTEC: A Source Term Code for High Level Nuclear Waste Geologic Repositories. Version 1.0. CNWRA92-009. San Antonio, TX: Center for Nuclear Regulatory Analyses (CNWRA).

Sharland, S.M., 1992. A mathematical model of the initiation of crevice corrosion in metals. *Corrosion Science* 33(2): 183-20

Shibata, T., and T. Takeyama. 1977. Stochastic theory of pitting. *Corrosion* 33: 243-25

Sridhar, N., G.A. Cragnolino, and W. Machowski. 1991. Environmental effects on localized corrosion of a high-level nuclear waste container material. T. Abrajano and L.H. Johnson, eds. *Materials Research Symposium Proceeding V.212. Scientific Basis for Nuclear Waste Management XIV.* Pittsburgh, PA: MRS: 269-277.

Sridhar, N., G.A. Cragnolino, H. Pennick, T.Y. Torng. 1991. Application of a transient crevice corrosion model to the prediction of performance of high-level nuclear waste container materials.

R.N. Parkins, ed. *Proceedings of a Conf. on Life Prediction of Corrodible Structures* Cambridge, England. To be Published by NACE.

Staehle, R.W. 1990. Understanding "situation dependent strength" a fundamental objective in assessing the history of stress corrosion cracking. *Proc. of the First International Conference on Environmental-Induced Cracking of Metals.* R.P. Gangloff and M.B. Ives eds. Houston, TX: NACE: 561-612.

Stewart, J. and D.E. Williams. 1992. The initiation of pitting corrosion on austenitic stainless steel: on the role and importance of sulfide inclusions. *Corrosion Science* 33 (3): 457-474.

Szklarska-Smialowska, Z. 1986. *Pitting Corrosion of Metals.* Houston, TX: NACE.

Tamaki, K., S. Tsujikawa, and Y. Hisamatsu. 1990. Development of a new test method for chloride stress corrosion cracking of stainless steel in dilute NaCl solutions. *Advances in Localized Corrosion.* H.S. Isaacs, U. Bertocci, J. Kruger, and S. Smialowska., eds. Houston, TX: NACE: 207-214.

Tsujikawa, S. and Y. Hisamatsu. 1984. Repassivation potential as a crevice corrosion characteristic for austenitic and ferritic stainless steels. Ya. M. Kolotyrkin, ed. *Proc. of Third Soviet-Japanese Seminar on Improvement of Corrosion Resistance of Structural Materials in Aggressive Media.* Moscow, Russia. Nauka Publishers:119-13

Tsujikawa, S., Y. Soné, and Y. Hisamatsu. 1987. Analysis of mass transfer in a crevice region for a concept of the repassivation potential as a crevice-corrosion characteristic. A. Turnbull, ed., *Corrosion Chemistry Within Pits, Crevices, and Cracks.* London. Her Majesty's Stationary Office:171-186.

Tsujikawa, S. and S. Okayama, 1990. Repassivation method to determine critical conditions in terms of electrode potential, temperature and NaCl concentration to predict crevice corrosion resistance of stainless steels. *Corrosion Science* 31:441-446.

Vetter, K.J. 1967. *Electrochemical Kinetics. Theoretical and Experimental Aspects.* New York, NY: Academic Press.

Walton, J.C. and B. Sagar. 1988. Modeling performance of steel containers in high-level waste repository environments: implications for waste isolation. *Radioactive Waste Management and the Nuclear Fuel Cycle.* 9(4):323-347.

Walton, J. 1992. *A Model for Transient diffusion, Electromigration, and Chemical Reaction in One Dimension - Version 1.0.* San Antonio, TX: CNWRA 92-019.

Wang, J.H., C.C. Su, and Z. Sklarska-Smialowska. 1988. Effects of Cl^- concentration and temperature on pitting of AISI 304 stainless steel. *Corrosion* 44(10):732-737.

Williams, D.E., C. Westcott, and M. Fleischmann. 1985a. Stochastic models of pitting corrosion of stainless steels. I. Modeling of the initiation and growth of pits at constant potential. *J. of Electrochemical Society* 132: 1796-1804.

Yashiro, H. and K. Tanno. 1990. The effect of electrolyte composition on the pitting and repassivation behavior of AISI 304 stainless steel at high temperature. *Corrosion Science* 31:485-490.

Yashiro, H., K. Tanno, H. Hanayama, and A. Miura. 1990. Effect of temperature on the crevice corrosion of type 304 stainless steel in chloride solution up to 250°C. *Corrosion* 46(9):727-733.

Yashiro, H., S. Koshiyama, and K. Tanno. 1992. Critical pitting and crevice corrosion potentials of type 304 stainless steel in NaCl solutions at 423°K. *Corrosion Engineering* 40:9-18.

Yashiro, H. and K. Tanno. 1992. Critical combination of pH, chloride concentration and temperature for pit initiation on type 304 stainless steel. G.S. Frankel and R.C. Newman eds. *Critical Factors in Localized Corrosion.* Pennington, NJ: The Electrochemical Society (TES): 460-468.

Zimmerman, R.M., R.L. Schuch, D.S. Mason, M.L. Wilson, M.E. Hall, M.P. Board, R.P. Bellman, and M.P. Blanford. 1986. *Final Report: G-Tunnel Heated Block Experiment.* SAND84-2620. Albuquerque, NM: Sandia National Laboratories (SNL).